Kinetic Analysis of the Regulation of the Na^+/H^+ Exchanger NHE-1 by Osmotic Shocks†

Jérôme Lacroix,[‡,⊥,#] Mallorie Poët,[‡,#] Laurence Huc,[§,▽] Vincent Morello,[¶] Nadir Djerbi,[‡] Michel Ragno,[‡] Mary Rissel,[§] Xavier Tekpli,[§] Pierre Gounon,[||] Dominique Lagadic-Gossmann,[§] and Laurent Counillon*[,‡]

Université de Nice-Sophia Antipolis, CNRS FRE3093 Transport Ionique aspects normaux et pathologiques, Faculté des Sciences Parc Valrose, 06108 Nice cedex 2, France, UPRES EA SERAIC, Université de Rennes I, Faculté de Pharmacie, 2 Avenue du Pr. Léon Bernard, 35043 Rennes Cedex, France, and Centre Commun de Microscopie Appliquée, Faculté des Sciences, Parc Valrose 06108 Nice cedex 2 France

Received July 22, 2008; Revised Manuscript Received November 1, 2008

ABSTRACT: NHE-1 is a ubiquitous, mitogen-activatable, mammalian Na^+/H^+ exchanger that maintains cytosolic pH and regulates cell volume. We have previously shown that the kinetics of NHE-1 positive cooperative activation by intracellular acidifications fit best with a Monod−Wyman−Changeux mechanism, in which a dimeric NHE-1 oscillates between a low- and a high-affinity conformation for intracellular protons. The ratio between these two forms, the allosteric equilibrium constant L_0, is in favor of the low-affinity form, making the system inactive at physiological pH. Conversely the high-affinity form is stabilized by intracellular protons, resulting in the observed positive cooperativity. The aim of the present study was to investigate the kinetics and mechanism of NHE-1 regulation by osmotic shocks. We show that they modify the L_0 parameter (865 ± 95 and 3757 ± 328 for 500 and 100 mOsM, respectively, vs 1549 ± 57 in isotonic conditions) This results in an activation of NHE-1 by hypertonic shocks and, conversely, in an inhibition by hypotonic media. Quantitatively, this modulation of L_0 follows an exponential distribution relative to osmolarity, that is, additive to the activation of NHE-1 by intracellular signaling pathways. These effects can be mimicked by the asymmetric insertion of amphiphilic molecules into the lipid bilayer. Finally, site-directed mutagenesis of NHE-1 shows that neither its association with membrane PIP_2 nor its interaction with cortical actin are required for mechanosensation. In conclusion, NHE-1 allosteric equilibrium and, thus, its cooperative response to intracellular acidifications is extremely sensitive to modification of its membrane environment.

NHE-1,[1] an isoform of the Na^+/H^+ exchanger family of integral membrane transporters, is expressed at the plasma membrane of all mammalian cells (for review see refs (*1*) and (*2*)). It belongs to a gene family whose members show sequence conservation throughout all phyla, highlighting the physiological importance of this transmembrane protein for all living cells and organisms.

NHE-1 uses the energy provided by the transmembrane sodium gradient to exchange a single intracellular H^+ ion against an extracellular Na^+. This exchanger, which is nearly inactive at physiological intracellular pH, becomes rapidly activated with increasing cytoplasmic acidity, reaching full activity in about 1 pH unit. This positive cooperativity constitutes an efficient molecular switch for regulating intracellular pH. In terms of biological engineering, this striking feature requires the existence of (i) at least two different conformations for the intracellular proton transport site that may be different in their maximal transport rates, affinities for protons, or both and (ii) at least two distinct binding sites for protons. These two interrelated properties can be obtained basically by two different mechanisms:

(i) The existence of a site, that binds but does not transport protons and which, depending on its state of protonation, can modify the affinity or the rate of the transport site (*3, 4*).

(ii) By two transport sites, which can change conformations in a concerted manner, thus modifying either affinities or rates of transport.

Although intuitive, the first model was not supported by a detailed kinetic analysis of transporters activation by

† This work was supported by the CNRS, the University of Nice-Sophia Antipolis, and the Fondation de France, Programme Recherche Cardiovasculaire.

* Corresponding author. Phone: 33 4 92 07 68 53. Fax: 33 4 92 07 68 50. E-mail: counillo@unice.fr.

‡ Université de Nice-Sophia Antipolis.

⊥ Present address: Department of Biochemistry and Molecular Biology, GCIS Building, Room W244, 929 E. 57th Street, Chicago, IL 69637.

# Both authors contributed equally to this work.

§ Université de Rennes I.

▽ Present address: INRA UMR1089 180 Chemin de Tournefeuille St Martin du Touch, BP3, 31931 Toulouse Cedex, France.

|| Centre Commun de Microscopie Appliquée.

¶ Present address: IPMC, CNRS UMR 6097, 660 Route Des Lucioles, 06560 Valbonne France.

[1] Abbreviations: BCECF/AM, (2′,7′-bis(carboxyethyl)-5,6-carboxyfluoresceine/acetoxy methylester); BSA, bovine serum albumin; ERM, ezrin/radixin/moesin protein family; FCS, fetal calf serum; HEPES, *N*-2-hydroxyethylpiperazine-*N*′-2-ethanesulfonic acid; MES, 2-(*N*-morpholino)ethanesulfonic acid; MOPS, 3-(*N*-morpholino)propanesulfonic acid; mOsM: mosmol/L; NHE-1, Na^+/H^+ exchanger isoform 1; pHi, intracellular pH; PIP_2, phosphatidylinositol (4,5)-bisphosphate; SEM, scanning electron microscopy; TEM, transmission electron microscopy.

10.1021/bi801368n CCC: $40.75
Published on Web 11/26/2008

intracellular protons (*5*). By contrast, the second model of concerted mechanism, in which proton binding sites undergo conformation changes that modify their affinities (i.e., a Monod−Wyman−Changeux model; for review, see ref *6*) fits remarkably well with the sigmoidal activation of NHE-1. In this mechanism, the transporter exists as a dimer in the plasma membrane and oscillates between a low- and a high-affinity form with respect to intracellular protons. The fact that the Monod−Wyman−Changeux equation fits the experimental data for a dimeric transporter fulfills the requirement of two distinct proton binding sites for cooperativity, with no requirement for a supplementary sensor site for protons. Such a dimer has been observed experimentally (*7*−*9*). In this mechanism, the major form of NHE-1 is the low-affinity exchanger, meaning that the system is almost totally off at neutral intracellular pH, as it is indeed the case. Intracellular acidification would shift the equilibrium toward the high-affinity form, which would then be stabilized by intracellular protons (*5*). This simple model of NHE-1 cooperative regulation, which fits the experimental data, is described by a set of only three constants: the two affinity constants for intracellular protons and the thermodynamic equilibrium constant associated with the allosteric transition, that is, L_0, the ratio of the low-affinity form to the high-affinity form. The situation is therefore quite different from the bacterial Na^+/H^+ exchanger Nha A, which exhibit a stoichiometry of two transported H^+ for one Na^+ and a strong negative cooperativity, with a Hill coefficient close to −3 for the dimeric form and about −2 for the monomeric form (*10*). These values require multiple proton binding sites in the same monomer within a dimer. This is supported by structural data, molecular simulations, and site-directed mutagenesis (*11, 12*). The similarities and differences between eukaryotic and prokaryotic exchangers may therefore constitute an area worthy of investigation.

In addition, we show that the Monod−Wyman−Changeux mechanism provides a molecular explanation for two other important modes of regulation of the exchanger, that is, NHE-1 growth factor activation and NHE-1 regulation by its membrane environment. Growth factors lead to both covalent and noncovalent modifications of the C-terminal regulatory region of NHE-1 via intracellular signaling pathways (for review, see ref *2*). This, increases the gain of the sigmoidal activation of NHE-1 by intracellular pH and fits with a decrease in L_0 and conversely with an increase in the level of the high-affinity form of NHE-1 for protons. Interestingly, the deletion of the C-terminal tail of NHE-1 leads to a noncooperative form of exchanger with a Hill coefficient of 1. Thus, this region of the protein, which is distinct from the transport domain, fulfills the role of an allosteric regulatory domain, such as that found in enzymes that follow the Monod−Wyman−Changeux model of positive cooperativity (*13*). In good accordance with this model, the group of Shigeo Wakabayashi found that these C-terminal tails are in close contact in the dimer and that, conversely, the disruption of this interaction decreases the cooperativity of NHE-1 response (*9*). Other mutations in the transport part of NHE-1 are also able to abolish this cooperative behavior, indicating that, as expected, several loops of the transport domain participate in this allosteric coupling. In a second study (*14*), we examined the influence of cholesterol- and caveolin-rich microdomains on NHE-1 activity. We observed that cholesterol depletion agents activated NHE-1 by decreasing its L_0 parameter, which was reverted by cholesterol repletion. This activation was associated with NHE-1 relocation outside microdomains and was additive to growth factor activation, which did not change NHE-1 localization. Thus, the localization of NHE-1 in membrane cholesterol- and caveolin-rich microdomains constitutes a negative constraint of NHE-1 activity, which enables the activation of this transporter by other stimuli (*14*).

Using an elegant technique of patch clamp adapted to pH measurements, Fuster et al. have shown in a pioneer work that NHE-1 is a mechanosensitive transporter affected by membrane tension and that the addition or removal of various lipids that modify the membrane curvature and tension change the activity of NHE-1 (*15*). To obtain further insights into this mechanism of action, we decided to explore how osmotic shocks, which modifiy membrane tension, affect the kinetic properties of the transporter. For this purpose, we measured initial rates of cariporide-sensitive $^{22}Na^+$ fluxes on fibroblasts expressing either wild-type or mutated NHE-1 and submitted to various osmotic shocks or changes in membrane lipid composition. The data obtained from these experiments were then used to determine how membrane tension affects the parameters defined by the Monod−Wyman−Changeux mechanism that describes NHE-1 response to intracellular pH.

MATERIALS AND METHODS

Cell Culture and Transfection. Exchanger-deficient fibroblasts from the PS120 cell line (*16*) were grown in Dulbecco's modified Eagle medium supplemented with 50 μg/mL streptomycin, 50 unit/mL penicillin, and 7.5% fetal calf serum at 37 °C in a humidified atmosphere of 5% CO_2 and 95% air. Transfections were performed using Fugene 6 (Roche), as described by the manufacturer. Cell populations stably expressing either wild-type or mutant NHEs were selected using 500 μg mL^{-1} G418 for 3 weeks before use. All experiments were systematically performed using cell population instead of clones in order to minimize variations that could have occurred between individual clones.

Measurement of Initial Rates of Na^+/H^+ Exchange. Unless stated otherwise, all of the experiments presented in this work were performed with cells maintained in 1% fetal calf serum for 16−18 h before measurements. These conditions maintain a basal level of NHE-1 activation that allows the measurement of both increases and decreases of the cooperative response to protons. Growth factor activation was measured by the addition of 20% fetal calf serum 15 min before the acidification.

Cells seeded on 24-well plates were acidified using the following protocol: they were incubated for 10 min in a sodium-free solution containing 2.5 μM nigericin (Sigma), 140 mM KCl, and adjusted to pH values in the range of 5.2−7.2 using HEPES, MOPS, or MES buffers (20 mM) as appropriate. Following 5 min incubation in the same solution in which the nigericin had been replaced by 50 mg mL^{-1} of BSA, the cells were quickly rinsed twice in (i) 120 mM choline chloride, 1 mM $CaCl_2$, 1 mM $MgCl_2$, 5 mM glucose, buffered at pH 7.0 with 10 mM HEPES (isotonic medium), (ii) 20 mM choline chloride, 1 mM $CaCl_2$, 1 mM $MgCl_2$, 5 mM glucose, buffered at pH 7.0 with 10 mM HEPES

(hypotonic medium), or (iii) 120 mM choline chloride, 1 mM $CaCl_2$, 1 mM $MgCl_2$, 5 mM glucose, buffered at pH 7.0 with 10 mM HEPES and supplemented with mannitol (hypertonic medium). Because of their low or Michaelian activities in isotonic conditions, the responses of the PIP_2/ERM mutants to membrane tension were tested using an osmolarity of 1200 mOsM.

For wild-type NHE-1, linear sodium uptake was carried out for 30 s in the same choline chloride media containing 0.25 μCi mL^{-1} $^{22}Na^+$. Uptake was stopped by four rapid rinses in ice-cold PBS. Cells were solubilized in 0.1 N NaOH, and radioactivity was measured by scintillation counting. Initial NHE-1 rates were calculated based on the cariporide-sensitive accumulation of $^{22}Na^+$. Because of their "Michaelian" behavior, mutants in the ERM and PIP_2 sites were characterized using 1 μCi of $^{22}Na^+$ and 5 min uptake in isotonic conditions.

Intracellular pH Fluorescence Measurements. Fibroblasts were acidified at pH 6.6 using the same nigericin protocol as described above: they were incubated for 10 min in a sodium-free solution containing 2.5 μM nigericin (Sigma), 140 mM KCl, and adjusted to pH 6.6 in the presence of 20 mM MES buffer (*5*). The acidified cells were incubated for 5 min with 5 μM of the pH-sensitive dye BCECF/AM and were then rinsed using the same solution as above. After 30 s, fibroblasts were perfused for 60 s with sodium-free solutions containing different concentrations of mannitol to reach the desired osmolarities (100 and 500 mOsM). To check for cellular integrity and NHE-1 functionality, pH recoveries were then triggered by the addition of an isotonic solution containing 120 mM NaCl.

In all these steps, which were performed at 37 °C, pH variations were monitored by measuring BCECF/AM fluorescence. The imaging system consisted of a Zeiss ICM 405 inverted microscope with a Zeiss 40× objective, coupled to a video camera. Fluorescence excitation was provided by a 75 W xenon lamp (Osram) and was computer-controlled by a shutter. The excitation beam was filtered through 450 and 490 nm narrow band interference filters paired with appropriate quartz neutral-density filters mounted in a computer-controlled motorized wheel. Cells were excited successively at 490 and 450 nm, and each image was digitized and stored on the computer hard disk. Image treatment was performed using the Axon Imaging Workbench software. Fifteen to twenty fibroblasts were usually used in each experiment.

At the end of the experimental series, the fluorescence signals relative to pHi were calibrated using the K^+/H^+ exchanging ionophore nigericin. For this purpose, the cells were perfused with a solution of 140 mM KCl, 20 mM HEPES, and 2.5 μM nigericin adjusted to pH 7. The pHi values for each individual cell were obtained by linear interpolation of the gray level values, and the calculated values were adjusted to between 6.6 (pH value at the beginning of the experiment) and 7 according to the experimental calibration. Individual pHs were then averaged for each individual experiment, which were then compiled for each condition.

Electron Microscopy. Following 15−30 s osmotic shocks, cells were fixed *in situ* at room temperature with 1.6% glutaraldehyde in 0.1 M phosphate buffer at pH 7.5. For SEM, cells were postfixed with 0.5% osmium tetroxyde and 0.5% potassium ferricyanide in 0.1 M cacodylate buffer, dehydrated with ethanol, and treated with hexamethyldisilazane before air drying. Samples were coated with 3 nm gold−palladium and observed with a Jeol 6400F scanning electron microscope. For TEM, cells were first postfixed with 1% osmium tetroxyde and 1% potassium ferricyanide to enhance the contrast in the cytoplasmic membranes and were then rinsed with distilled water, dehydrated with ethanol, and finally embedded in Epon. Thin sections were contrasted with uranyl acetate and lead nitrate and observed with a Philips CM12 transmission electron microscope operating under standard conditions.

NHE-1 Quantitation and Trypsin Accessibility Assay. NHE-1 mature and immature forms were quantified in the different conditions using Western blotting followed by densitometric analysis with respect to actin as a loading control using ImageJ software (Rasband W.S., NIH, Bethesda MD). The presence of the mature form of NHE-1 at the plasma membrane was determined by exposing the cells for 60 s to extracellularly applied trypsin (Invitrogen BRL) at 0.5 mg/mL in hypotonic, isotonic or hypertonic media at room temperature, as describes in ref *14*. Briefly, following osmotic shocks, cells were exposed to 0.5 mg/mL trypsin for 60 s at room temperature and rinsed twice with ice-cold PBS supplemented with 5% BSA. Crude membranes were then prepared. The different forms of NHE-1 (mature, cleaved, and immature), either under control conditions or following shocks, were visualized by Western blotting using an antibody against the C terminal end of NHE-1 normalized against actin (Millipore).

Lithium Uptake. In order to obtain an independent direct measurement of the velocities of Na^+/H^+ exchange, we designed lithium uptake measurements, which can provide a direct estimation of the cation flux mediated by the NHE-1. Cells were acidified by a 1 h incubation in 50 mM NH_4Cl, 90 mM NaCl, 5.4 mM KCl, 1 mM $CaCl_2$, 1.2 mM $MgCl_2$, 11 mM glucose, buffered at pH 7.4 with 10 mM HEPES, followed by two rapid rinses in the choline chloride solution fixed at different osmolarities using mannitol (see previous section). Under these conditions, intracellular pH dropped to the estimated value of 5.2, as calibrated using nigericin (*14*). Cells were then incubated in the same solutions as above supplemented with 3 mM LiCl for 1 min.

Lithium uptake was then stopped by four rapid rinses in ice-cold phosphate buffered saline (PBS). Cells were solubilized in 1 N nitric acid (trace metal grade HNO_3, Sigma), and the intracellular lithium was measured using atomic absorption spectrometry using a Zeeman furnace system (Solaar 969, Thermo Optek). NHE-1 initial rates were calculated as the cariporide (10 μM)-sensitive Li^+ accumulation per well divided by the corresponding protein concentration.

Modification of the Membrane Using Crenator and Cup Formers. The effect of crenators and cup formers was determined by treating cells for 20 min with 200 μM arachidonate or 10 μM chlorpromazine (Sigma), respectively, before the acidification step. Before use, the arachidonate was dissolved in ethanol and the chlorpromazine in 90% H_2O/10% ethanol.

Site-Directed Mutagenesis. The amino acid sequence of the first PIP_2/ERM site, ^{513}KKKQETKR^{520} was changed to MIMQETML, and the amino acid sequence of the second PIP_2/ERM site, ^{556}RFNKKYVKK^{564}, was changed to LFNHIYVHH, both using double-stranded mutagenesis (Quick-

Change site-directed mutagenesis, Stratagene). The different steps were performed as described by Poët et al. (*17*) using oligonucleotides bearing the appropriate codon changes (MWG Biotech) on a 1.6 kb *Sac*I−*Eco*RI cDNA cassette subcloned into pBSK, which contained the sites of interest. The sequences of the 5′ to 3′ oligonucleotide coding strands were gttggctgtgatgataatgcaagagacgatgctctccatcaacg and gctcaacctgtttaatatgatatatgtgatgatgtgtctgatagc for the first and second PIP_2/ERM mutants, respectively. After sequencing, the mutated cassette was reintroduced by restriction cutting and subsequent religation into the modified polycistronic pECE-IRES vector (SV40 promoter) containing the NHE-1 cDNA (*5*). Before transfection, the mutated constructs were again tested by restriction analysis and automated sequencing (GenomeExpress). The presence of the appropriate mutations was also verified in the stably transfected cell lines by PCR amplification of genomic DNA and subsequent sequencing.

Data Analysis and Treatment. Data were compiled using Microsoft Excel software and fitted using the Sigmaplot 2001 program (Jandel) with built-in or user-defined equations that are provided in the Results section or Supporting Information. Unless stated otherwise, the experimental points correspond to the compilation of at least five independent experiments, with each experimental point determined at least in duplicate. All experimental points are provided with standard error of the mean for error bars. Constants obtained from fitting our data, given in the text or the tables, are provided with the error of the fits and r^2 goodness-of-fit factors.

RESULTS

Modulation of the NHE-1 Allosteric Response by Osmotic Shocks. The cariporide-sensitive rapid uptake of $^{22}Na^+$ was measured at different intracellular pH values that were precisely clamped using the nigericine acidification technique described by Lacroix et al. (*5*) and for different osmolarities, as described in Materials and Methods. The measured sodium fluxes were totally blocked by the specific NHE-1 inhibitor cariporide and were also undetectable in exchanger-deficient PS120 cells (data not shown). In these experiments, only the initial rates of NHE-1 activity were measured to permit the precise determination of the allosteric parameters of NHE-1. Figure 1 shows that the shape of the sigmoidal dose−response curve of NHE-1 was modified at different intracellular pH values in response to variations in osmotic pressure. Specifically, hypertonic shocks increased NHE-1 sensitivity to intracellular acidification, while hypotonic shocks produced the opposite effect.

Osmotic Shocks on NHE-1 Transfected Fibroblasts. In order to verify that this effect was not due to nonspecific effects that would affect the cells as a whole instead of NHE-1, we decided to explore in further detail the effect of the osmotic shocks on the fibroblasts used for our measurements.

In Figure 2A−E, fibroblasts seeded on 35 mm plates were exposed to osmotic shocks (100 or 500 mOsM) in the absence of extracellular sodium or bicarbonate to block any possible effects of the Na^+-dependent and independent HCO_3^- transport mechanisms on the regulation of cell volume or pH (see Materials and Methods). In Figure 2A,B, intracellular pH variations were followed using the BCECF fluorescent probe, while in Figure 2D,E osmotic shock-induced morphological changes were visualized by electron

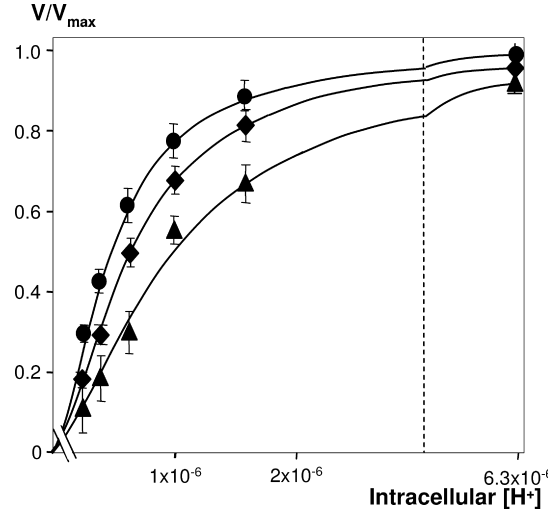

FIGURE 1: Modulation of NHE-1 activity by osmotic shocks. Cells expressing WT NHE-1 seeded on 24-well plates were maintained in 1% FCS for 16−18 h and then acidified at different intracellular pH values as described in Materials and Methods. Initial rates of NHE-1 activity were determined by measuring fast $^{22}Na^+$ uptake conducted at desired osmolarities using different concentrations of mannitol (▲, 100 mOsM; ◆, 300 mOsM; ●, 500 mOsM). Plots represent V/V_{max} values against intracellular H^+ concentration. Data are representative for at least seven independent experiments. Error bars are standard error of the mean. Note the increase in the NHE-1 cooperative response in hypertonic conditions and its decrease in hypotonic conditions.

microscopy in comparison with control fibroblasts (Figure 2C). In the fluorescence measurements, intracellular pH was clamped at a value of 6.6 using nigericin acidification (see Materials and Methods) and then followed during the osmotic shocks. After 60 s of shock, the cells were exposed to an isotonic solution containing 120 mM NaCl. The observed pH recovery slopes (Figure 2A,B) indicated that the cells were fully functional after the osmotic shocks, which did not significantly alter the intracellular pH.

Figure 2C−E show the surfaces of the cells (SEM) and details of their membrane morphologies (TEM) in isotonic medium and following the hypertonic and hypotonic shocks. Whereas the overall sizes and shapes of the cells did not vary noticeably between the two conditions, the membrane features were very different. Exposure to hypotonic shock did not produce global swelling, but instead created local dilatations, resulting in folds along the main axes of the cells. Hypertonic shocks, on the other hand, did not result in global shrinking, but rather produced a flattened membrane punctuated with villosity. Interestingly, in isotonic medium an intermediate state can be observed in which cells bear both visible lines in the same orientation as the above-mentioned folds as well as sparse villosity. Taken together, the results presented in Figure 2 indicate that over the short time course of the experiments, osmotic shocks did not simply shrink or swell the cells but instead modified the membrane features, maybe by expanding morphological motives (folds and villi) that are already present but less pronounced in isotonic conditions.

NHE-1 Quantitation, Trypsin Accessibility, and Maximal Rates of Exchange. Another important control was to verify that the observed changes in activity were not due to modifications of NHE-1 quantities at the plasma membrane leading proportionally to decreases in maximal rate (V_{max})

that is embedded in the Monod−Wyman−Changeux equation (see below). This was investigated by semiquantitative Western blots in which we used densitometric analysis to verify that the shocks did not modify the ratios of mature and immature forms of NHE-1 versus an actin loading control. We also verified the expression of the NHE-1 mature form at the plasma membrane using trypsin accessibility assays in hypo-, iso-, and hypertonic conditions, as described in ref *14*. In a second step, we developed an assay based on lithium uptake measurement to monitor NHE-1 activity directly and independently from the $^{22}Na^{+}$ uptake measurements. As shown from the data in Figure 3, neither hypo- nor hypertonic conditions elicited any changes in the total amounts of NHE-1. As expected, at the very acidic pH values produced by the ammonium prepulse acidification technique, where NHE-1 is very close to V_{max}, hypertonic shocks could not further increase NHE-1 activity (Figure 3B) showing no effect of osmotic pressure on V_{max}, while hypotonic shocks produced a slight decrease.

The Response of NHE-1 to Osmotic Shocks Involves Changes in the Allosteric Constant L_0. The data obtained in Figure 1 were fitted to the Monod−Wyman−Changeux equation for a dimeric NHE-1 (*5*) as given below (eq 1):

$$V/V_{max} = \bar{Y} = \frac{\alpha(1+\alpha) + L_0 c\alpha(1+c\alpha)}{L_0(1+c\alpha)^2 + (1+\alpha)^2} \quad (1)$$

where $\alpha = [H^+]/K_h$, $c = K_h/K_l$, K_h = the microscopic affinity of the high-affinity form, K_l = the microscopic affinity of the low-affinity form, and L_0 = [low-affinity form]/[high-affinity form]. This yielded excellent fits with the observed modifications of the L_0 allosteric constant and good fits with the microscopic constants of the high- and low-affinity forms for protons, K_h and K_l, as variables (Table 1, Supporting Information). To discriminate between these two possible mechanisms involving either a modification of the allosteric equilibrium or modification(s) of the affinities of the two forms we used the R327E mutant, which is shifted toward the low-affinity form in isotonic conditions (*5*) and displays Michaelian behavior, with a K_m for intracellular protons corresponding to the low-affinity constant of the system. As shown in Figure 4, this mutant is still able to regain cooperativity in hypertonic conditions (Hill coefficient = 1.2 ± 0.07), meaning that the osmolarity changes are not exerting their effects by modifying the proton affinity of the protein. Two completely independent mutants described at the end of this study display a similar phenotype. Taken together, these results show that the regulation of NHE-1 by osmotic

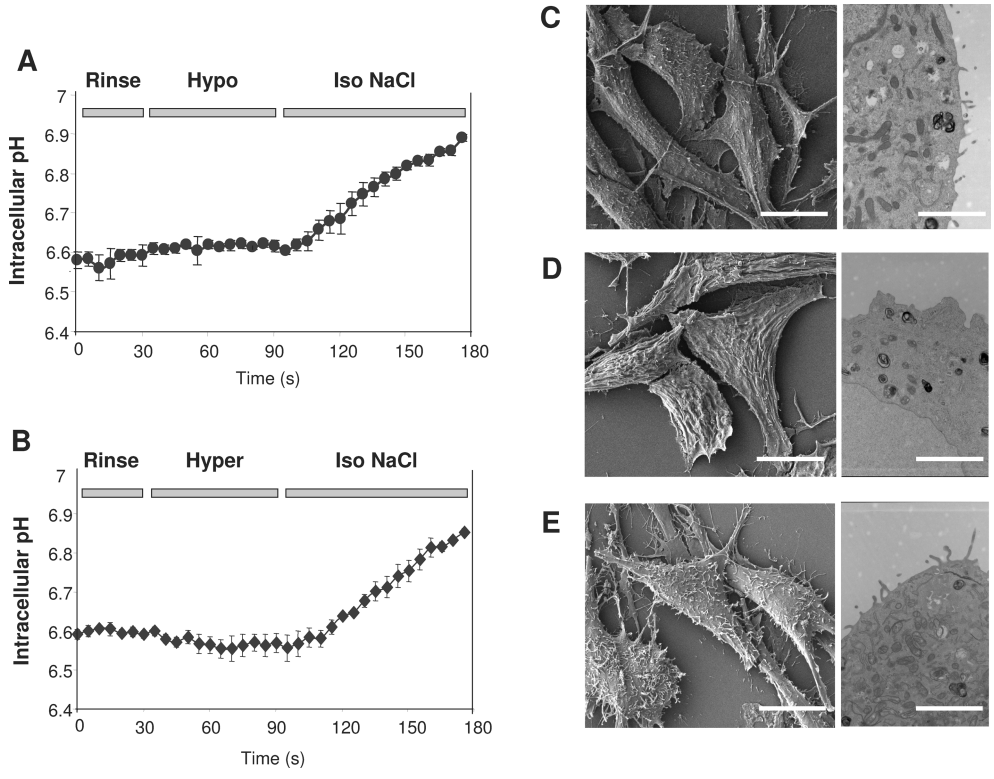

FIGURE 2: Osmotic shocks on NHE-1 transfected fibroblasts. (A, B) Intracellular pH: Cells expressing NHE-1 were loaded with the pH sensitive dye BCECF/AM. At the beginning of the experiments, intracellular pH was clamped at 6.6 using the nigericin acidification technique described in Materials and Methods. After 30 s in sodium- and bicarbonate-free medium (rinse medium, see Materials and Methods), the cells were perfused with either hypotonic (Hypo, 100 mOsM, panel A) or hypertonic (Hyper, 500 mOsM, panel B) sodium-free solutions for 60 s. Cells were then perfused with an isotonic bicarbonate-free solution containing 120 mM NaCl (Iso NaCl) to visualize NHE-1 activity. The experimental points on the graphs correspond to the average of at least five independent experiments with 15−20 cells in each experiment. The error bars correspond to standard error of the mean. (C) Morphological SEM and TEM analysis of fibroblasts in isotonic conditions: NHE-1 transfected PS120 fibroblasts were treated for electron microscopy analysis as described in Materials and Methods. Scale bars are 10 μm (SEM, left) and 2.5 μm (TEM, right). (D) Morphological SEM and TEM analysis of fibroblasts submitted to a hypotonic shock: NHE-1 transfected PS120 fibroblasts were submitted to a 100 mOsM medium for 15 s and treated for electron microscopy analysis as described in Materials and Methods. Scale bars are 10 μm (SEM, left) and 2.5 μm (TEM, right). (E) Morphological SEM and TEM analysis of fibroblasts submitted to a hypertonic shock: NHE-1 transfected PS120 fibroblasts were submitted to a 500 mOsM medium for 15 s and treated for electron microscopy analysis as described in Materials and Methods. Scale bars are 10 μm (SEM, left) and 2.5 μm (TEM, right).

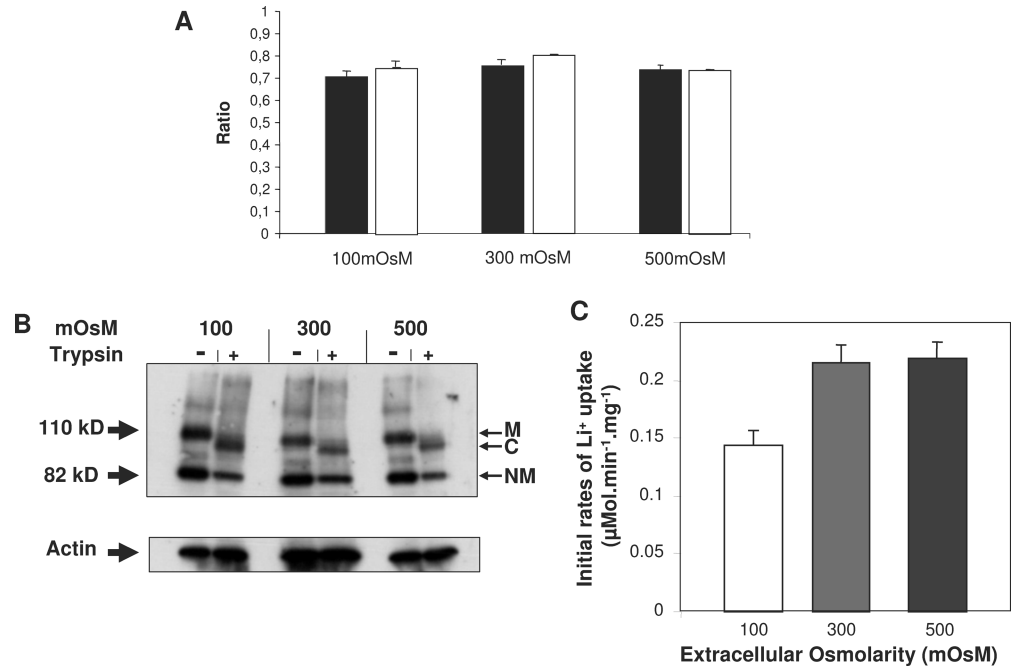

FIGURE 3: NHE-1 membrane expression and activity. (A) NHE-1 transfected PS120 fibroblasts were submitted to 100, 300, or 500 mOsM for 30 s. Crude membranes were then prepared. Proteins were then separated by SDS−PAGE. The different forms of NHE-1 and actin were visualized by Western blotting and quantified using densitometric analysis. The histogram represents the ratio of NHE-1 mature (dark bars) and immature forms (white bars) versus actin, which was used as a loading control. (B) NHE-1 transfected PS120 fibroblasts were submitted to 100, 300, or 500 mOsM for 30 s. Trypsin was then added externally at a final concentration of 0.5 mg/mL for 60 s at room temperature and stopped by two rinses with ice-cold PBS supplemented with 5% BSA. Crude membranes were then prepared. The different forms of NHE-1 (M for mature, C for cleaved, and NM for immature) were separated by SDS−PAGE and visualized by Western blotting. (C) NHE-1 transfected fibroblasts were acidified to pH 5.2, and NHE-1 activity was monitored by measurement of initial rates of lithium (1 mM extracellular concentration) uptake for 1 min in hypo-, iso-, or hypertonic conditions. After four rapid rinses in ice-cold PBS, cells were lysed in nitric acid, and intracellular lithium concentrations were measured using atomic absorption spectroscopy.

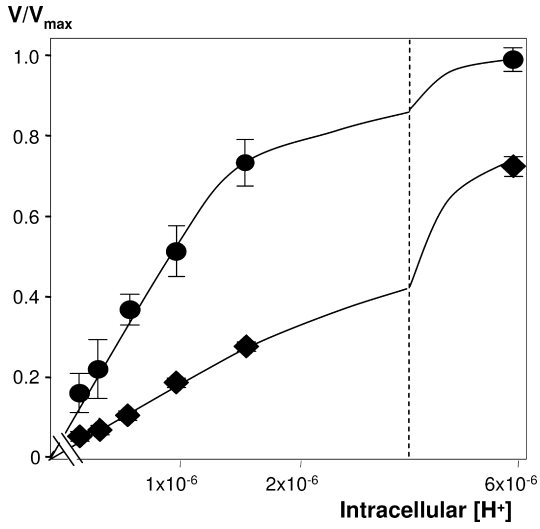

FIGURE 4: Response of the R327E mutant to osmotic shocks. Cells expressing the R327E mutant seeded on 24-well plates were maintained in 1% FCS for 16−18 h and then acidified at different intracellular pH values. Initial rates of NHE-1 activity were determined by measuring fast $^{22}Na^+$ uptake conducted either in isotonic or in hypertonic conditions (◆, 300 mOsM; ●, 1200 mOsM). Plots represent V/V_{max} values against intracellular H^+ concentration. Data are representative for at least five independent experiments. Error bars are standard error of the mean. Note that this mutant displays a Michaelian response to intracellular acidification and regains cooperativity upon hypertonic shocks.

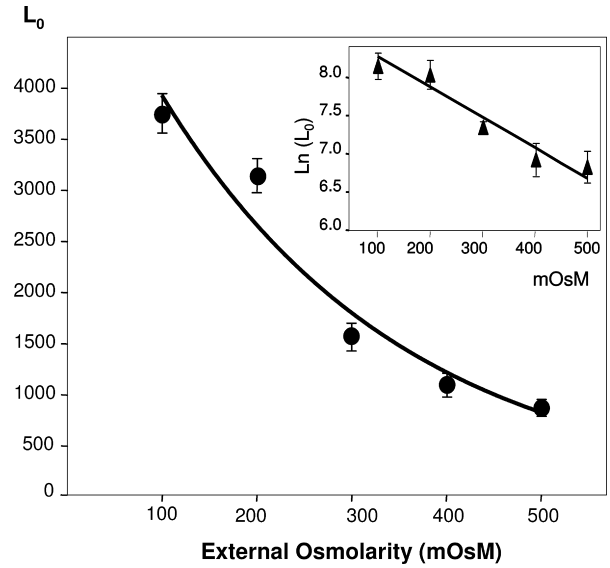

FIGURE 5: Relation between NHE-1 allosteric constant and osmolarity. The fractions of maximal NHE-1 activity (V/V_{max}) were measured in cells maintained in 1% FCS for different intracellular pH values at different external osmolarities, using the same experimental protocol as in Figure 1. The values of the allosteric parameter L_0 were determined from the V/V_{max} plots at each osmolarity value using the Monod−Wyman−Changeux equation for a dimeric NHE-1. Error bars correspond to errors of the fits, which were obtained from at least five experiments at each osmolarity. The plots were fitted with a single exponential. The inset shows the linear regression of the plot obtained using the logarithm of L_0.

shocks is best explained by a modulation of the allosteric constant L_0 of the system.

Relationship between NHE-1 Allosteric Constant and Osmolarity. Figure 5 shows the L_0 values plotted against different osmolarity values applied to the membrane of cells maintained in 1% FCS. This curve fits best with an

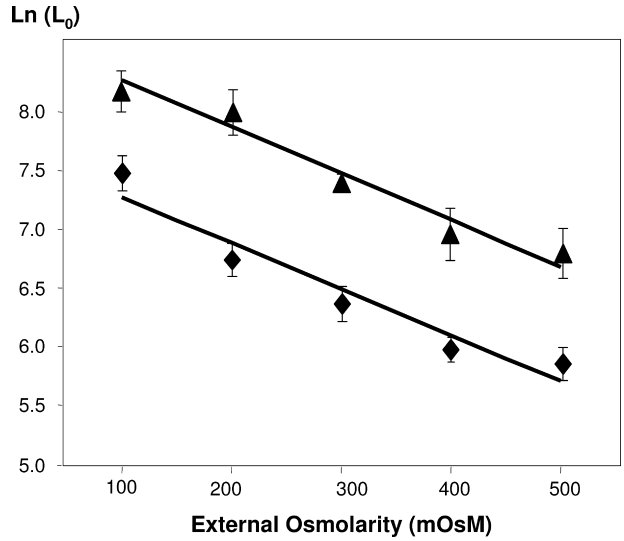

FIGURE 6: Comparison of NHE-1 regulation by serum and osmotic shocks. The graph shows the linear regression of L_0 values plotted against differences in osmolarities between the extracellular and intracellular compartments in 20% (◆) or 1% (▲) fetal calf serum. Cells expressing WT NHE-1 were maintained in 1% fetal calf serum for 16−18 h. Twenty minutes before the experiment, the medium was changed to a bicarbonate-free HEPES-buffered medium supplemented with either 20% FCS (◆) or 1% FCS (▲). NHE-1 activities were then measured for osmolarities ranging from 100 to 500 mOsM. NHE-1 activity was then determined by $^{22}Na^+$ uptake. The value of the allosteric parameter L_0 was calculated with the Monod−Wyman−Changeux equation from the experimental V/V_{max} data. Data for stimulated cells are representative for at least seven independent experiments. Error bars are as in Figure 3.

exponential distribution and, conversely, can be linearized using the logarithm of L_0 (Figure 5, see inset, rsq = 0.96). A more detailed analysis of all the components of the distribution reveals that the data can equally be fitted with sums of exponentials. However, this treatment does not significantly improve the goodness of the fits (for example, rsq = 0.953 for three exponentials). We therefore chose to use the simplest equation giving the best fits, that is, a single exponential.

The logarithm of the exponential distribution of L_0 versus osmolarity gives a straight line ($\ln(L_0) = (a + b\text{OsM})/(kT)$). Its slope ($-3.99 \times 10^{-3} \pm 4.6 \times 10^{-4}$ mOsM^{-1}) provides a quantitative estimation of the sensitivity of the allosteric response of the transporters to the osmolarity applied to the cell.

Quantitation of NHE-1 Response to Osmotic Shocks. We then characterized the response of NHE-1 to osmotic shocks after 15 min stimulation with 20% FCS. Serum was used in this particular case because of its ability to activate signaling pathways in a pleiotropic manner. As shown in Figure 6, this yielded a line that was parallel to that obtained from the above-mentioned set of experiments in 1% serum. Linear regression gave nearly identical slope coefficients: $-3.99 \times 10^{-3} \pm 4.6 \times 10^{-4}$ mOsM^{-1} in unstimulated cells (rsq = 0.96) versus $-4.19 \times 10^{-3} \pm 4.39 \times 10^{-4}$ mOsM^{-1} (rsq = 0.92) in cells stimulated with 20% serum. These results indicate that the mitogenic activation of the cells affected the basal set point of NHE-1 sensitivity to intracellular protons but did not modify the sensitivity of the exchanger's allosteric equilibrium to osmotic pressure.

Modification of the NHE-1 Allosteric Equilibrium by Crenators and Cup Formers. Cells were incubated for 20 min with either 200 μM arachidonate, which inserts preferentially into the external leaflet of the membrane, or 10 μM chlorpromazine, which inserts preferentially into the inner leaflet (*18, 19*). Figure 7A,B shows the effects of these molecules on the cells and the morphological features of their membranes, as visualized by SEM or TEM. As can be seen in the kinetic measurements presented in Figure 7C, arachidonate decreases NHE-1 sensitivity to internal protons, while chlorpromazine exerts the opposite effect. Fitting these data gave L_0 values of 8518 ± 1106 (rsq = 0.988) for arachidonate and 811 ± 43 for chlorpromazine (rsq = 0.995), compared with L_0 = 1549 ± 57 (rsq = 0.998) in the control conditions. These data are summarized in Table 1.

Potential Sites of NHE-1 Modulation by Osmotic Pressure. The C-terminal regulatory region of NHE-1 possesses two positively charged stretches of amino acids that correspond to PIP$_2$/ERM binding domains. The first site is situated between positions 513 and 520 (sequence KKKQETKR), and the second site is more distal, located between positions 556 and 564 (sequence RFLKKYVKK). These sites have been shown to bind both the inner leaflet phospholipid PIP$_2$ (*20*) and the actin cytoskeleton (*21*). These two domains are good candidates for segments acting to transduce pressure to NHE-1 because they connect the regulatory region of the transporter to both the membrane and the actin cytoskeleton.

We eliminated the first site by removing all of its positively charged amino acids that bind PIP$_2$ through electrostatic interaction using site-directed mutagenesis (MIMQETML sequence). This produced a strongly defective phenotype, in good accordance with results obtained by Aharonowitz et al. (*21*). We were unable to detect any significant activity of this mutated exchanger in isotonic conditions. Interestingly, activity was restored in hypertonic conditions (1200 mOsM), although the mutant protein showed no detectable cooperative kinetics (L_0 > 29000, see Figure 8A) and exhibited Michaelian behavior with an affinity constant for protons close to the K_m value of the low-affinity exchanger (K_m = 3.17 ± 0.98 μM, rsq = 0.997).

We next eliminated the second site by substituting all of its lysines and arginines (sequence LFNHIYVHH). When tested for its kinetic parameters, this mutant showed a drastic loss of cooperativity. Fitting these data with a hyperbolic curve yielded a K_m value similar to that of low-affinity NHE-1 forms (3.92 ± 0.67 μM, rsq = 0.979) previously obtained using independent mutations (*5*). We next investigated whether this mutated exchanger was still allosterically activatable by osmotic shock. Figure 8B shows that hypertonic shocks (1200 mOsM) could indeed activate this mutant, which regained cooperative activation by intracellular pH with an L_0 value of 2898 ± 405 (rsq = 0.975).

Because both mutants still responded to osmotic shocks, we constructed a double mutant by successive site-directed mutagenesis of the two above-mentioned sites using the same oligonucleotides and stably expressed the construct in PS120 cells. As shown in Figure 8C, this double mutant displayed a very similar phenotype to the second PIP$_2$/ERM mutant, in terms of both activity and its response to hyperosmolarity.

In addition we estimated the sensitivity of the two single and double mutants to osmotic pressure by measuring initial rates of Li^+ uptake (see Materials and Methods) at 500 and 1200 mOsM and plotting the results as the ratio to the control conditions. As shown in Figure 8 D, all three mutants

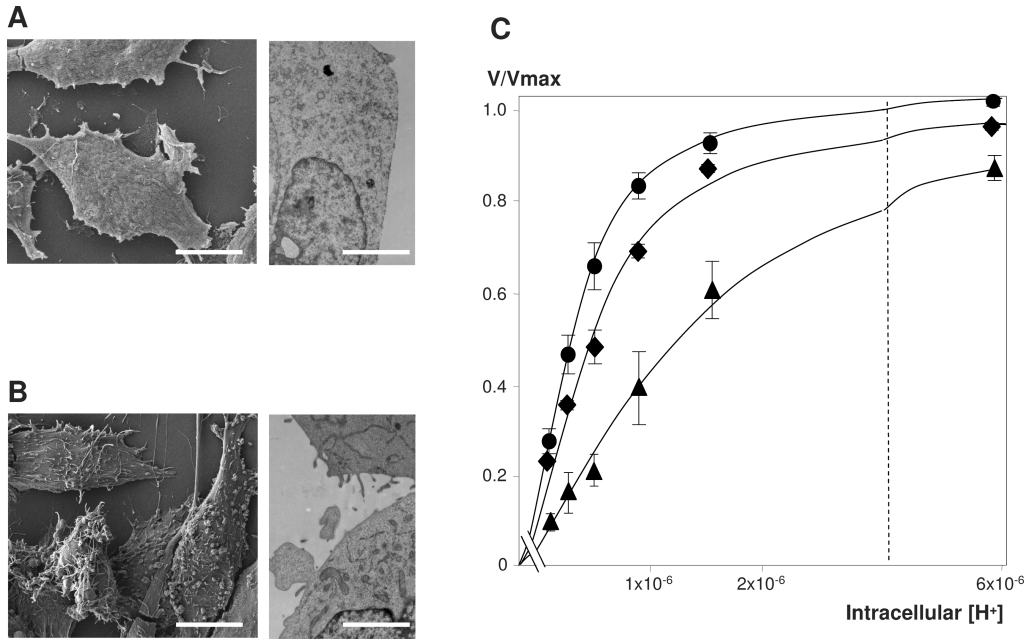

FIGURE 7: Effects of arachidonate and chlorpromazine. (A) Morphological SEM and TEM analysis of fibroblasts submitted to 200 μM arachidonate. NHE-1 transfected PS120 fibroblasts were incubated with 200 μM arachidonate for 20 min and then treated for electron microscopy analysis as described in Materials and Methods. Scale bars are 10 μm (SEM, left) and 2.5 μm (TEM, right). (B) Morphological SEM and TEM analysis of fibroblasts submitted to 10 μM chlorpromazine. NHE-1 transfected PS120 fibroblasts were incubated in 10 μM chlorpromazine for 20 min and then treated for electron microscopy analysis as described in Materials and Methods. Scale bars are 10 μm (SEM, left) and 2.5 μm (TEM, right). (C) Modulation of NHE-1 activity. Cells were treated with 10 μM chlorpromazine (CPZ, ●) or 200 μM arachidonic acid (▲) for 20 min in serum-free medium and acidified immediately after the treatment using the nigericin method. The graph represents V/V_{max} values plotted against intracellular H^+ concentration. Data are representative of at least three independent experiments. Note the allosteric activation of NHE-1 in the presence of CPZ and its allosteric inhibition in the presence of arachidonic acid, compared with the control curve. L_0 values obtained by fitting these curves using the Monod−Wyman−Changeux model are presented in Table 1.

Table 1: Values of the allosteric constant L_0 for Wild-Type and Mutated NHE-1 in Different Conditions[a]

	L_0	error	rsq
WT NHE-1			
1% FCS	1549	±57	0.998
20% FCS	583	±44	0.989
hypotonic shock (100 mOsM)	3757	±328	0.993
hypertonic shock (500 mOsM)	867	±95	0.976
chlorpromazine	811	±43	0.995
arachidonic acid	8518	±1106	0.988
R327E			
hypertonic shock (1200 mOsM)	1761	396	0.955
PiP_2/ERM Site 1			
1% FCS	*b*	*b*	*b*
hypertonic shock (1200 mOsM)	>100000	*b*	*b*
PiP_2/ERM Site 2			
1% FCS	>30000	*b*	*b*
hypertonic shock (1200 mOsM)	2898	±405	0.975

[a] Each L_0 value corresponds to at least three measurements for each experimental point performed at least in duplicate. The errors and goodness of the fit parameter (rsq) are shown in the table. [b] Not determined.

strongly responded to osmolarity. Taken together, these phenotypes show that neither the connection between NHE-1 and membrane PIP_2 nor that between the protein and the cortical actin cytoskeleton are required for the sensitivity of NHE-1 to osmotic pressure.

DISCUSSION

The aim of the present work was to study how osmotic pressure quantitatively modifies the kinetics of NHE-1. For this purpose, we used fast measurements of cariporide-sensitive $^{22}Na^+$ uptake at clamped intracellular pH in the absence of bicarbonate. This experimental approach was designed to combine the advantages of a reconstituted system, in which the important parameters can be controlled, with being as close as possible to the features of a cellular system, in which the protein is maintained in its physiological context in terms of membrane environment, associated proteins, signaling pathways, and cytoskeleton.

NHE-1 allosteric response was characterized using the set of three quantitative parameters defined by the Monod−Wyman−Changeux equation: an equilibrium constant (L_0) and two affinity constants (K_h, and K_l) for the two conformations of the proton binding sites within the dimeric NHE-1.

Figure 1 shows that hypertonic shocks increase the gain of the sigmoidal response of NHE-1 to intracellular protons, making the exchanger more active for a given pH, while in the other direction hypotonic shocks allosterically inhibit the transporter. This symmetry suggests that the mechanism by which osmotic pressure modulates NHE-1 might be of a physical nature rather than involving a complex interplay of signaling cascades. A large set of controls was used to rule out nonspecific effects that would indirectly affect the measured parameters (Figures 2 and 3).

The data shown in Figure 1 gave excellent fits with changes in L_0 values and good fits with changes in the microscopic affinity constants (Supporting Information) of the Monod−Wyman−Changeux equation. Thus these kinetic data by themselves do not enable discrimination between two very different mechanisms, either a modification of the allosteric equilibrium of the transporter or a modification of

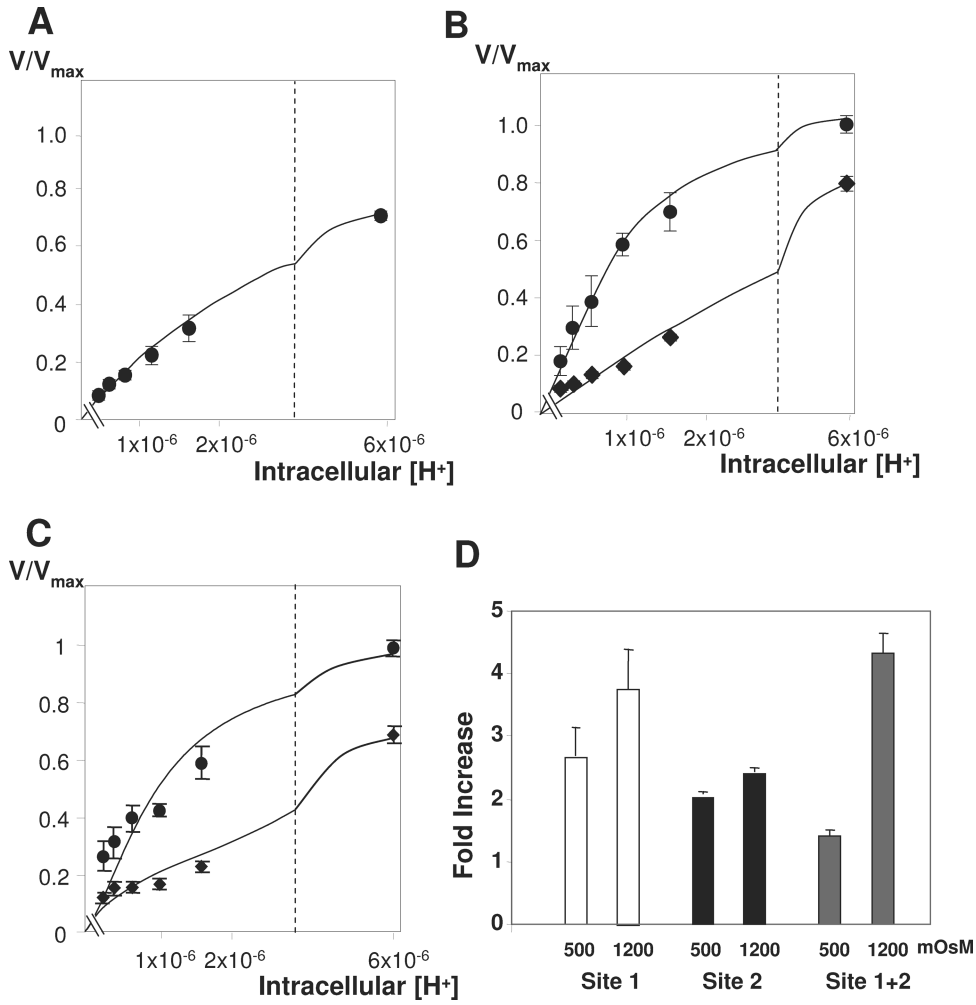

FIGURE 8: PIP_2/ERM binding sites and response to osmotic shocks. (A) First PIP_2/ERM binding site of NHE-1. Cells expressing the first PIP_2/ERM binding site NHE-1 mutant (^{513}KKKQETKR^{520} sequence changed to MIMQETML) were incubated in a 1% FCS medium for 16−18 h before the experiment. Cells were then acidified according to the nigericin procedure and rinsed twice in sodium-free medium, either isotonic or adjusted in 1200 mOsM with mannitol. The cooperative response of this mutant was then measured as V/V_{max} by $^{22}Na^+$ uptake for a range of different intracellular H^+ concentrations. Data are representative of at least six independent experiments. The curve corresponding to the isotonic extracellular medium is not shown because no significant $^{22}Na^+$ accumulation was detected in these conditions. Note that in the strongly hypertonic conditions used in this set of experiments the curve has a hyperbolic shape. (B) Second PIP_2/ERM binding site of NHE-1. Cells expressing the second PIP_2/ERM site NHE-1 mutant (^{556}RFNKKYVKK^{564} sequence changed to LFNHIYVHH) were incubated in culture medium containing 1% FCS for 16−18 h before the experiment. Cells were then acidified following the nigericin method and rinsed twice in serum-free media adjusted to 300 (◆) or 1200 mOsM (●). The activity of the second PIP_2/ERM NHE-1 mutant was determined as V/V_{max} values with the fast $^{22}Na^+$ for the different intracellular pH values. Data are representative of at least five independent experiments. Error bars correspond to standard error of the mean. Note the hyperbolic dependence of the curve in isotonic conditions and its allosteric shape in hypertonic conditions. (C) The double mutant for the two PIP_2/ERM binding sites of NHE-1. Cells expressing the double mutant affecting the two PIP_2/ERM binding sites (see above) were incubated in culture medium containing 1% FCS for 16−18 h before the experiment. Cells were then acidified according to the nigericin method and rinsed twice in serum-free media adjusted to 300 (◆) or 1200 mOsM (●). The activity of the double PIP_2/ERM mutant was determined as V/V_{max} values with the fast $^{22}Na^+$ for the different intracellular pH values. Data are representative of at least four independent experiments. Error bars correspond to standard error of the mean. (D) Relative sensitivities of the two single and the double mutant to either 500 and 1200 mOsM. Initial rates of Na^+/H^+ exchange were measured for either 500 or 1200 mOsM conditions. Fold increases calculated as ratios to the activity in isotonic conditions are represented to provide an estimation of the sensitivity of the mutants to osmolarity.

its intrinsic affinities for intracellular protons. To answer this question, we took advantage of the Michaelian R327E mutant (*5*), which is shifted toward the low-affinity form of the exchanger. If the mechanism involved a change in L_0, exposure to a hypertonic medium would be expected to restore the cooperative kinetics of the exchanger. By contrast, if the mechanism involved changes in the intrinsic affinities of the exchanger, the medium would change the K_m of the mutant for protons (see Supporting Information section 2 for more details on the possible mechanisms and their implications). As shown in Figure 4, exposure of this mutant to a hypertonic medium resulted in the restoration of cooperative kinetics. Two independent mutants also presented in this study showed similar phenotypes, providing independent confirmation of this observation. Taken together, these results cannot be explained by a model in which microscopic affinities for protons are modified. Instead, NHE-1 regulation by osmotic shocks occurs through the modulation of the allosteric equilibrium of the system, characterized by the parameter L_0.

The plot of L_0 at different osmolarities fits with an exponential distribution (Figure 5) that is similar to Poisson−Boltzmann distribution of the open probability of

mechanosensitive channels that switch between open and closed states at different osmotic pressures (*22*) (eq 2):

$$P_0 = 1/[1 + e^{(a+b\Pi)/(kT)}] \quad (2)$$

where P_0 = the open probability of a channel that oscillates between an open and a closed state following a simple equilibrium, Π = the pressure applied to the membrane, and T = the temperature. The a and b constants are phenomenological coefficients specific to the channel's response.

This equation is identical to one describing an exponential curve for an equilibrium constant instead of an open probability ($L_0 = e^{(a+b\Pi)/(kt)}$). Interestingly, the slope of the linear representation of the logarithm of L_0, provides a quantitative estimation of the sensitivity of NHE-1 to osmotic pressure (Figure 5, inset). When measured between serum-starved cells (1% serum) and cells stimulated with 20% fetal calf serum, this sensitivity did not change. Thus, while the activation of signaling pathways shifts the basal allosteric equilibrium of NHE-1, it does not significantly modify the sensitivity of NHE-1 to osmolarity.

If the above-mentioned results are correct, amphiphillic molecules that modify membrane tension and curvature and conversely NHE-1 activity (as shown by Fuster et al. (*15*)) are expected to modify NHE-1 cooperative response to protons in a similar manner as osmotic shocks. Such molecules, termed crenators and cup formers, have been used in the characterization of mechanosensitive potassium channels in both prokaryotic (*18*) and eukaryotic organisms (*19*). Although the correspondence between the membrane deformation induced by the asymmetric insertion and the amount of pressure applied in adherent cells is complex compared with the pioneer studies in erythrocytes (*23*), the electron microscopy observations presented in Figure 7A,B show that arachidonate and chlorpromazine modify the cellular and membrane morphological features in a manner reminiscent of the changes triggered by osmotic shocks (Figures 2D,E). As shown in Figure 5C, these compounds produced the shifts in the dose−response curves of NHE-1 response to intracellular protons, mimicking osmotic shocks. More importantly, the observed shifts fitted extremely well with modification in the L_0 parameter, which is also modified by osmotic shocks. Taken together, these results provide a quantitative mechanism of the effects of a whole range of fatty acids on NHE-1 (*15, 28*; Supporting Information section 3 and Poet, M., and Counillon, L. unpublished results). They have also to be considered in connection with our recent results concerning the inhibitory effect of the presence of NHE-1 in cholesterol-rich microdomains in the membrane (*14*). In this context, we have also verified that osmotic shocks do not modify NHE-1 localization or the cholesterol content of the microdomains (Supporting Information section 4). Finally, we also tried to combine the effects of osmotic shocks and modification of the membrane environment using either arachidonate, chlorpromazine, or cholesterol depletion (Supporting Information section 5). No significant change could be detected from these modifications in hypotonic conditions. The fact that arachidonate failed to further inhibit NHE-1 in these conditions clearly confirms that this fatty acid does not act as a classical inhibitor but that its effect is linked to membrane constraints. This is also confirmed by the fact that arachidonate decreases the V_{max} but not the K_m of NHE-1 for sodium (Supporting Information section 3) By contrast and as expected, the activation of NHE-1 by hypertonic shocks can be partially blocked by arachidonate and increased by chlorpromazine and cholesterol depletion.

To summarize, our results confirm that NHE-1 is a mechanosensitive transporter and show the mechanism of its sensitivity to osmotic pressure is the modulation of the allosteric equilibrium constant (L_0). This can be mimicked by other modifications of the membrane in isotonic conditions.

The last part of this study was aimed at exploring the sites within NHE-1 that could be involved in its sensitivity to membrane tension. Because the cytosolic C-terminal region of the protein works as an allosteric regulatory domain (*5, 20, 24*), we investigated whether it contains obvious sites that could physically connect NHE-1 to the plasma membrane or to membrane-associated proteins. No myristoylation or palmitoylation consensus sites, which could covalently link NHE-1 to the membrane, were evident in this part of NHE-1. By contrast, two sequence stretches bearing extensive positive charges have been documented in the first part of the NHE-1 C-terminus that can connect the protein to membrane PIP_2 and to cortical actin via members of the ERM family (*20, 21, 25*). These sites are reported to be essential not only for the optimal activity of NHE-1 but also for important cellular functions such as cell adhesion and motility (for review, see ref *21*), as well as AKT-dependent cell survival (*26*). The first site is very close to the end of the transmembrane region of NHE-1, at position 515. A similar sequence is found at a similar position in the mechanosensitive 2P potassium channel TREK 1 (*27*). We eliminated these two sites by site-directed mutagenesis, which was preferred over PIP_2 depletion or F-actin disruption in wild-type cells because using these inhibitors we observed what we interpreted as non-specific side effects on cell membranes or shape that could indirectly affect the NHE-1 response (data not shown). Both of these mutations had a strong impact on the allosteric behavior of NHE-1 in isotonic conditions. The site 1 mutant displayed a very low activity in $^{22}Na^+$ uptake experiments (Figure 8A). Because we could still detect the mature plasma membrane form of the mutant in Western blots at wild-type levels, we concluded that eliminating this site did not affect the stability or expression of the protein but rather impeded its ability to fold properly or to catalyze ion exchange. By contrast, the second site mutant displayed Michaelian behavior, with an affinity constant for protons of close to 3 μM (Figure 8B). Interestingly, both mutants could be activated by hypertonic shocks. The exposure of the first site mutant to hyperosmolarity had an interesting effect: it restored the activity of NHE-1 but in the absence of any clear allosteric behavior (Figure 8A). We propose that the hyperosmolarity-induced membrane constraints act on the mutated exchanger in a manner that restores its ability to transport ions but fails to restore its allosteric regulation. The site 2 mutant clearly showed an allosteric response (Hill coefficient of 1.25 ± 0.06), with an L_0 value of 2898 ± 405 (Figure 8B). This is very similar to the behavior of the completely independent R327E mutant and confirms that the sensitivity of NHE-1 to membrane tension is due to the modulation of its allosteric constant. Surprisingly, the double mutant (Figure 8C) showed a restoration of its cooperative regulation despite the loss of the two sites. Interestingly the two single and the double mutant showed

a greater potency to be activated by hypertonic shocks than the wild-type exchanger (Figure 1 and Figure 8D). However, this result has to be interpreted with caution because these mutants have a much lower activity than the wild-type NHE-1 in isotonic conditions, making their activation comparatively greater with respect to the basal state. Nevertheless, the data obtained from these mutants rule out the possibility that the interaction of NHE-1 with membrane PIP_2 or with the actin cytoskeleton is necessary and sufficient to mediate the protein's response to mechanical forces.

To summarize, the functional effects of NHE-1 interaction with cytoskeletton and membrane are complex. This strongly suggests that unidentified domains of the transporter participate in regulation by osmotic pressure. A simplifying hypothesis would be that the membrane directly acts on the packing of the transmembrane portion of NHE-1, which shares a large part of its external hydrophobic surface with the lipid environment. Another interesting possibility could be that other cytoskeletal elements, such as microtubules participate in this regulation (*29*).

Taken together, the results presented in this study show that a complex mechanism of regulation can be analyzed in a simple, coherent, and quantitative manner using the Monod−Wyman−Changeux model. Osmotic pressure or membrane modification regulates the cooperative response of NHE-1 to intracellular proton by modifying the energy balance and thus the equilibrium constant between the two forms of the transporter.

ACKNOWLEDGMENT

We thank Drs. Bruno Antonny, Eric Honoré, Anne-Odile Hueber, and Amanda Patel for fruitful discussions and Peter Follette for editorial work on the manuscript.

SUPPORTING INFORMATION AVAILABLE

Table summarizing the fits of the Monod−Wyman−Changeux equation for a dimeric NHE-1 with the microscopic affinities of the two forms taken as variables, diagram showing the analysis of the different possibilities for allosteric modulation of the R327E and ERM binding mutants by membrane tension, evidence that other fatty acids than arachidonate are pH-dependent noncompetitive inhibitors of NHE-1, V_m value and apparent K_m for sodium following the incubation with arachidonate, evidence that osmotic shocks do not modify the distribution of cholesterol and of NHE-1 in microdomains, combination of Osmotic shocks with lipid modification, Western blot of the wild-type and the three mutant exchangers. This material is available free of charge via the Internet at http://pubs.acs.org.

REFERENCES

1. Orlowski, J., and Grinstein, S. (2004) Diversity of the mammalian sodium/proton exchanger SLC9 gene family. *Pflugers Arch. 447*, 549–565.
2. Counillon, L., and Pouyssegur, J. (2000) The expanding family of eucaryotic Na(+)/H(+) exchangers. *J. Biol. Chem. 275*, 1–4.
3. Aronson, P. S., Nee, J., and Suhm, M. A. (1982) Modifier role of internal H^+ in activating the Na^+-H^+ exchanger in renal microvillus membrane vesicles. *Nature 299*, 161–163.
4. Wakabayashi, S., Hisamitsu, T., Pang, T., and Shigekawa, M. (2003) Kinetic dissection of two distinct proton binding sites in Na^+/H^+ exchangers by measurement of reverse mode reaction. *J. Biol. Chem. 278*, 43580–43585.
5. Counillon, L., Lacroix, J., Poet, M., and Maehrel, C. (2004) A mechanism for the activation of the Na/H exchanger NHE-1 by cytoplasmic acidification and mitogens. *EMBO Rep. 5*, 91–96.
6. Changeux, J. P., and Edelstein, S. J. (2005) Allosteric mechanisms of signal transduction. *Science 308*, 1424–1428.
7. Fafournoux, P., Noel, J., and Pouysségur, J. (1994) Evidence that Na^+/H^+ exchanger isoforms NHE-1 and NHE3 exist as stable dimers in membranes with a high degree of specificity for homodimers. *J. Biol. Chem. 269* (4), 2589–2596.
8. Vinothkumar, K. R., Smits, S. H., and Kuhlbrandt, W. (2005) pH-induced structural change in a sodium/proton antiporter from Methanococcus jannaschii. *EMBO J. 24*, 2720–2729.
9. Hisamitsu, T., Pang, T., Shigekawa, M., and Wakabayashi, S. (2004) Dimeric interaction between the cytoplasmic domains of the Na+/H+ exchanger NHE-1 revealed by symmetrical intermolecular cross-linking and selective co-immunoprecipitation. *Biochemistry 43*, 11135–11143.
10. Rimon, A., Tzubery, T., and Padan, E. (2007) Monomers of the NhaA Na+/H+ antiporter of *Escherichia coli* are fully functional yet dimers are beneficial under extreme stress conditions at alkaline pH in the presence of Na+ or Li+. *J. Biol. Chem. 282* (37), 26810–26821.
11. Hunte, C., Screpanti, E., Venturi, M., Rimon, A., Padan, E., and Michel, H. (2005) Structure of a Na^+/H^+ antiporter and insights into mechanism of action and regulation by pH. *Nature 435*, 1197–1202.
12. Arkin, I. T., Xu, H., Jensen, M. Ø., Arbely, E., Bennett, E. R., Bowers, K. J., Chow, E., Dror, R. O., Eastwood, M. P., Flitman-Tene, R., Gregersen, B. A., Klepeis, J. L., Kolossváry, I., Shan, Y., and Shaw, D.E. (2007) Mechanism of Na+/H+antiporting. *Science 317* (5839), 799–803.
13. Newton, C. J., and Kantrowitz, E. R. (1990) The regulatory subunit of *Escherichia coli* aspartate carbamoyltransferase may influence homotropic cooperativity and heterotropic interactions by a direct interaction with the loop containing residues 230−245 of the catalytic chain. *Proc. Natl. Acad. Sci. U.S.A. 87* (6), 2309–2313.
14. Tekpli, X., Huc, L., Lacroix, J., Rissel, M., Poët, M., Noël, J., Dimanche-Boitrel, M. T., Counillon, L., and Lagadic-Gossmann, D. (2008) Regulation of Na(+)/H(+) exchanger 1 allosteric balance by its localization in cholesterol- and caveolin-rich membrane microdomains. *J. Cell. Physiol. 216*, 207–220.
15. Fuster, D., Moe, O. W., and Hilgemann, D. W. (2004) Lipid- and mechanosensitivities of sodium/hydrogen exchangers analyzed by electrical methods. *Proc. Natl. Acad. Sci. U.S.A. 101* (28), 10482–10487.
16. Pouysségur, J., Sardet, C., Franchi, A., L'Allemain, G., and Paris, S. (1984) A specific mutation abolishing Na^+/H^+ antiport activity in hamster fibroblasts precludes growth at neutral and acidic pH. *Proc. Natl. Acad. Sci. U.S.A. 81*, 4833–4837.
17. Poet, M., Tauc, M., Lingueglia, E., Cance, P., Poujeol, P., Lazdunski, M., and Counillon, L. (2001) Exploration of the pore structure of a FMRF-amide gated-Na^+ channel. *EMBO J. 20*, 5595–5602.
18. Kloda, A., and Martinac, B. (2001) Mechanosensitive channel of *Thermoplasma*, the cell wall-less archaea: Cloning and molecular characterization. *Cell. Biochem. Biophys. 34*, 321–347.
19. Patel, A. J., Honore, E., Maingret, F., Lesage, F., Fink, M., Duprat, F., and Lazdunski, M. (1998) A mammalian two pore domain mechano-gated S-like K^+ channel. *EMBO J. 17*, 4283–4290.
20. Aharonovitz, O., Zaun, H. C., Balla, T., York, J. D., Orlowski, J., and Grinstein, S. (2000) Intracellular pH regulation by Na(+)/H(+) exchange requires phosphatidylinositol 4,5-bisphosphate. *J. Cell Biol. 150*, 213–224.
21. Denker, S. P., Huang, D. C., Orlowski, J., Furthmayr, H., and Barber, D. L. (2000) Direct binding of the Na-H exchanger NHE-1 to ERM proteins regulates the cortical cytoskeleton and cell shape independently of H(+) translocation. *Mol. Cell 6*, 1425–1436.
22. Markin, V. S., and Sachs, F. (2004) Thermodynamics of mechanosensitivity. *Phys. Biol 2*, 110–124.
23. Sheetz, M. P., and Singer, S. J. (1974) Biological membranes as bilayer couples. A molecular mechanism of drug-erythrocyte interactions. *Proc. Natl. Acad. Sci. U.S.A. 71*, 14457–14461.
24. Wakabayashi, S., Fafournoux, P., Sardet, C., and Pouyssegur, J. (1992) The Na^+/H^+ antiporter cytoplasmic domain mediates growth factor signals and controls "H(+)-sensing". *Proc. Natl. Acad. Sci. U.S.A. 89*, 2424–2428.

25. Baumgartner, M., Patel, H., and Barber, D. L. (2004) Na^+/H^+ exchanger NHE-1 as plasma membrane scaffold in the assembly of signaling complexes. *Am. J. Physiol. Cell. Physiol. 287*, 844–850.
26. Wu, K., Khan, S., Lakhe-Reddy, S., Jarad, G., Mukherjee, A., Obejero-Paz, C., Konieczkowski, M., Sedor, J. R., and Schelling, J. R. (2004) The NHE-1 Na^+/H^+ exchanger recruits Ezrin/Radixin/Moesin proteins to regulate Akt-dependent cell survival. *J. Biol. Chem. 279*, 26280–26286.
27. Chemin, J., Patel, A. J., Duprat, F., Lauritzen, I., Lazdunski, M., and Honore, E. (2005) A phospholipid sensor controls mechanogating of the K^+ channel TREK-1. *EMBO J. 24*, 44–53.
28. Goel, D. P., Maddaford, T. G., and Pierce, G. N. (2002) Effects of omega-3 polyunsaturated fatty acids on cardiac sarcolemmal Na(+)/H(+) exchange. *Am. J. Physiol Heart Circ. Physiol. 283* (4), H1688–H1694.
29. Elsing, C., Gosch, I., Hennings, J. C., Hübner, C. A., and Herrmann, T. (2007) Mechanisms of hypotonic inhibition of the sodium, proton exchanger type 1 (NHE-1) in a biliary epithelial cell line (Mz-Cha-1). *Acta Physiol. (Oxford) 190* (3), 199–208.

BI801368N